

Hail events in Germany, rare or frequent natural hazards?

Tabea Wilke, Katharina Lengfeld, and Markus Schultze

Deutscher Wetterdienst, Offenbach, Germany

Correspondence: Tabea Wilke (wilke.ta@t-online.de)

Abstract. Hail represents a natural hazard in Germany with potentially substantial economic and environmental impacts, but it often receives less attention than other weather phenomena. This, combined with the very local nature of hail, results in a lack of observations and further analysis. This study investigates hail characteristics, across Germany using crowdsourced observations since 2000 and weather radar data over a six year period. A study with 3D printed hailstones provided insights into human perception of hail sizes, revealing that collective crowd estimates closely approximate actual measurements, though individual estimations can vary significantly. By deriving hail proxies out of radar data we analyzed hail frequency, spatial distribution, and size variations. Our research reveals a gradient in hail occurrence, with southern Germany experiencing substantially higher hail probabilities compared to northern regions. Mountainous areas demonstrated increased hail frequency relative to lower-elevation territories. June emerged as the peak month for hail events, characterized by both highest frequency and largest hail sizes. This research contributes to a better understanding of hail as a natural hazard in Germany, providing valuable insights for risk assessment, insurance purposes, and public awareness.

1 Introduction

Hail is a major natural hazard that causes severe damage and high costs. Although hail is not the natural hazard with the highest damaging potential in Germany, it can lead to severe loss. A hailstorm in July 1984 in Bavaria led to insured damages of 1.5 Billion €, another event in July 2013 to 3.6 Billion € in Baden–Wuerttemberg and the most recent large hailstorm in June 2023 with 740 Mio € total loss are examples of very heavy, damaging hailstorms in Germany (dkk, 2021; gdv, 2023). On agriculture hail has the greatest impact during the growing season, whereby the actual damage depends on many factors such as hail size, crop type and growth condition (Sánchez et al., 1996). Further hail damage can be expected to the infrastructure.

Measuring and observing hail is a difficult task. There are different sources of hail observations: The human observations, indirectly through damages reported to the insurance companies, remote sensing, disdrometers and hailpads. Each of them has its own advantages and disadvantages. Human observations will always have the disadvantage of the spatial resolution. Most hail reports are made by people living in populous areas. Rural areas are very likely to be underrepresented. Thus, there is a reporting bias towards hail in cities and along roads (Allen and Tippet, 2015; McGovern et al., 2022). Further on, untrained reporters may have problems in estimating the size of hail (we further investigate this in Sec. 4.2). The last problem occurs in every measuring method of hail: it melts through falling and laying at the ground. That is one of the reasons why the exact size of a hailstone is hard to measure. It could also have an irregular shape, making sizing even more difficult.

For insurance data similar aspects are true as for human observation. It has a population bias and even a rich–poor bias, as the loss expense depends on the amount of insured property. The number of insured properties must also be accounted for. Another problem is the question of which hailstorms cause damage. Hohl et al. (2002) showed that the season must be included, as the high season produces less, but larger hailstones for the same kinetic energy than the low season. This is relevant for the mean damage, but has no noticeable influence on the total loss. Brown et al. (2015) highlight the need for diverse data that includes more than just weather, as the roof system is responsible for the most significant impact, accounting for 90 % of the total damage and this depends heavily on the material and the condition of the roofing system. The largest damages nevertheless do not correlate with the maximum hail size (Ackermann et al., 2023).

To overcome the issue of the population bias, weather radars can be a useful tool. They cover a large area and provide three dimensional data with high spatiotemporal resolution. We cannot derive hail size from radar data directly. Therefore, the challenge is finding a measure that is used as a proxy for hail and hail size. A first approach with single-polarized radars uses the reflectivity in combination with heights of specific temperatures which are derived from model data. Early on in hail research, Waldvogel et al. did a large study with hailpads to find a criterion for hail. They used the height of 45 dBZ (H_{45}) and the melting layer H_0 . The hail probability at the ground should hereby be proportional to the difference of heights. With this approach, the probability of hail (POH) is calculated with a stepwise function using the difference between H_{45} and H_0 , whereby POH gets larger with increasing difference. (Holleman et al., 2000; Witt et al., 1998; Nisi et al., 2016). The stepwise function was then adapted to a curve by Foote et al. (2005) and used e.g in Trefalt et al. (2022).

Another method to estimate the hailsize is the Maximum Estimated Size of Hail (MEHS/MESH) (Witt et al., 1998). MESH is based on the Severe Hail Index (SHI) that takes the vertical integrated kinetic energy above the melting layer into account. The SHI is fitted to observed data to come up with a formula to obtain the maximum hail size (Witt et al., 1998; Murillo and Homeyer, 2019). MESH was originally developed for S-band radars in the US, Brook et al. (2024) showed that MESH used with C-band radars tends to overestimate hail sizes compared to S-band radars. To overcome this issue, Brook et al. (2024) introduced an empirical correction based on the matching of S-band and C-band radars in overlapping regions. Forcadell et al. (2024) utilize convolutional neural networks (CNNs) to obtain MESH values due to threshold-based optimization. In this study, we undertook our own calibration of the MESH formula with hail reports compared to the SHI derived from German C-band radar values (Sec. 4.5).

The upgrade from single- to dual-polarized radar systems gives the opportunity to improve the estimation of hail size. Aydin et al. (1986) and Depue et al. (2007) suggest the hail differential reflectivity H_{DR} which combines the reflectivity Z and the differential reflectivity Z_{DR} . Ryzhkov et al. (2013), however, remark that the melting process of hail is neglected and propose a fuzzy-logic scheme that also includes the cross correlation ρ_{hv} additionally. ρ_{hv} is a measure of the uniformity of hydrometeors within a measured volume, large hail is expected to have lower ρ_{hv} values (Heinselman and Ryzhkov, 2006).

At Deutscher Wetterdienst vertically integrated ice (VII) has been utilized operationally for years in the context of detecting potential hail occurrences. Its value to hail size relationship was developed by forecasters. It is important to note that VII is not widely recognized for its capabilities in hail size estimation, which serves as a motivation for the present study.

A different approach tries to estimate updrafts. For the development of the potential of large hailstones it is necessary to have

strong updrafts. Z_{DR} columns, intend to estimate the presence and height of super-cooled water. It can provide information on the location and strength of updrafts (Snyder et al., 2015). Another hint for updraft dimensions and the potential of large hail generation is the Specific Differential Phase (K_{DP}) column (Snyder et al., 2017).

- 65 Puskeiler et al. (2016) and Puskeiler (2014) analyzed hail in Germany based on radar data with the cell tracking TRACE3D (Handwerker, 2002). Their hail climatology for Germany shows hotspots that are strongly linked to the orography. Junghänel et al. (2016) combined reported data with reflectivity values of radar data, either having a report and a reflectivity value higher than 50 dBZ or having a reflectivity value higher than 55 dBZ only. Similar results also based on radar data were found by Fluck et al. (2021). All the hail studies for Germany have the hotspot of hail in southern Baden–Wuerttemberg in common.
- 70 Further on, they share the north–south increase of hail days. This was also observed in model-derived hail days (Battaglioli et al., 2023).

In this paper we derive multi annual hail data (2018–2023) for Germany based on VII. We compare it to crowdsourced data and investigate their annual cycles and spatiotemporal frequencies. In a case study we depict the similarities and differences for different hail size estimation methods. We focus on two research questions:

- 75 – Can we rely on human observed hail data in their size estimation?
- Are the radar based algorithms VII and MESH suitable for determining hail (size) climatologies for Germany?

2 Data

2.1 Human observed data

For the human observed data there are three different data sources available in Germany: WarnWetter app, European Severe
80 Weather Database, manned weather stations.

The first source are user reports obtained with the WarnWetter app. The mobile phone application operated by Deutscher Wetterdienst (DWD) informs the public about the current and forecasted weather and provides weather warnings. The application enables users to submit reports on their observations of weather conditions as well as upload pictures. Upon reception, all user reports are quality checked with reference data e.g. radar data (Spitzer et al., 2023). Regarding hail, users can select between
85 the following: *Hagel unter 1 cm*, *Hagel 1 cm*, *Hagel 2 cm*, *Hagel 3 cm*, *Hagel 5 cm*, *Hagel größer 7 cm* (hail smaller 1 cm, hail 1 cm, hail 2 cm, hail 3 cm, hail 5 cm, hail larger 7 cm). The already quality checked reports are cleaned up for further analysis, so users who reported an event for a day no other user reported an event are blacklisted and for users, who reported more than one event in 30 minutes, only the report with the largest hail size is taken into account.

The European Severe Weather Database (ESWD) (Dotzek et al., 2009) was established in 2006. It contains data on severe
90 convective storm events contributed by the public (eyewitnesses and voluntary spotters) and is quality controlled. With an update in the year 2008 the quality control was further enhanced. It contains four steps, from basic plausibility checks to fully verified (Dotzek et al., 2009). In this analysis we use data with basic plausibility checks (QC0+). The first reports are available for 2000 even though the test phase of the ESWD had started in 2004. A severe hail event is characterized by a maximum hail

diameter larger than 2 cm. From 2021 on, some of the reports of the WarnWetter app are transferred to the ESWD. There is a
95 continuous increase in reports from 2000 until 2008 with a maximum of approximately 300 reports in a year. Compared to the
previous years, in which there was no major change, there was a drop of reports in the years 2014–2018 (160–200 reports per
year).

The largest dataset comes from station observations of the monitoring network operated by DWD. It combines manned weather
stations and trained volunteer reports. The temporal accuracy of those reports differs from daily reports up to the exact time
100 of the hail event. In order to combine them, only the reported day of occurrence is taken into account. Due to the continuous
automation of weather observations, the number of reports decreases with time. For this reason the dataset only contains data
up to 2017.

The problem of point observation data is the low and irregular spatial resolution. Rural areas might be underrepresented due to
the lack of people who can report an event. Thus, the crowdsourcing data can only provide information about positive events,
105 as no report does not automatically mean no hail. The station observations, however, can also give a hint about the absence of
hail.

All in all, there are 3769 hail reports in the ESWD from 2000 to 2020. All reports independent of their quality level (QC0+ and
higher) were used in our study. Further on, the reports of hail of the new DWD WarnWetter app were used (since 2021). They
are automatically checked for plausibility and partially included in the ESWD dataset, amounting to 39 142 reports. Inclusion
110 in the ESWD involves a manual check of the content and plausibility of the reports for hail sizes greater than 2 cm. Hail sizes
smaller than 2 cm are not included. To ensure no duplicates were included in our analysis, ESWD data from 2021 and newer
was excluded. The smallest category “Hagel unter 1 cm” (hail smaller 1 cm) was left out in the analysis due to the possibility
to mistakenly reporting graupel instead of hail. With that, 21 231 reports remained in the analysis from the WarnWetter app.
For the years 2000–2017, 25 719 reports of the station observations of the DWD are available. In total the analysis includes 50
115 719 hail reports.

2.2 Radar data

The German radar network consists of 17 C-band doppler radars and covers whole Germany and adjacent areas (see Fig.
1). Upgrading single- to dual-polarization radars was started in 2011 and finished in 2021. Each radar provides scans in 11
elevation angles every 5 minutes (see Fig. 2).

120 The volume scan has a range of 180 km. The precipitation scan, a low-elevation scan that follows the orography, covers a range
of 150 km. Both scan types have a horizontal resolution of $1^\circ \times 250$ m.

In this study, we will evaluate the years 2018-2023, with a particular focus on the convective season between April to
September.

2.3 Insurance data

125 The federation of private insurance companies in Germany, the *German Insurance Association* (GDV), has kindly provided
access to their hail damage data, with hail and storm forming one category. The decision for a category “hail”, “storm” or

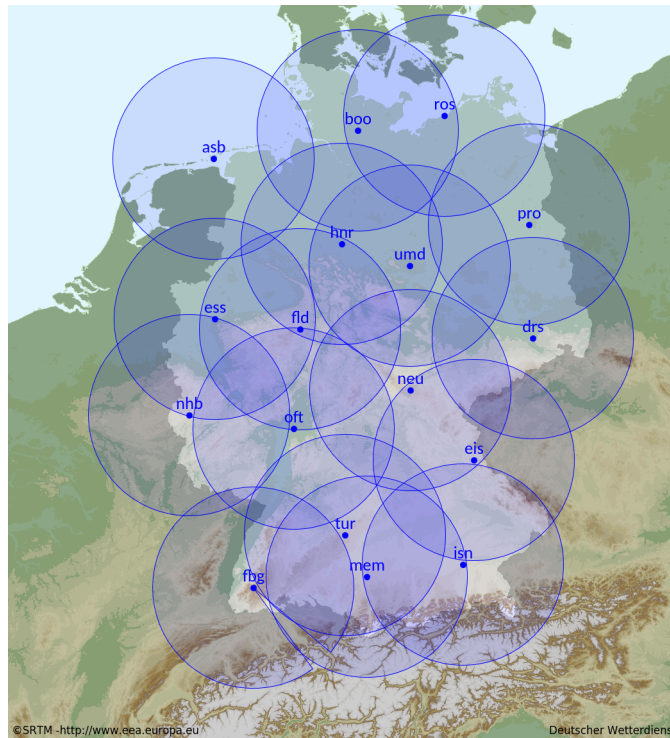


Figure 1. The German radar network with its 17 C-band radars.

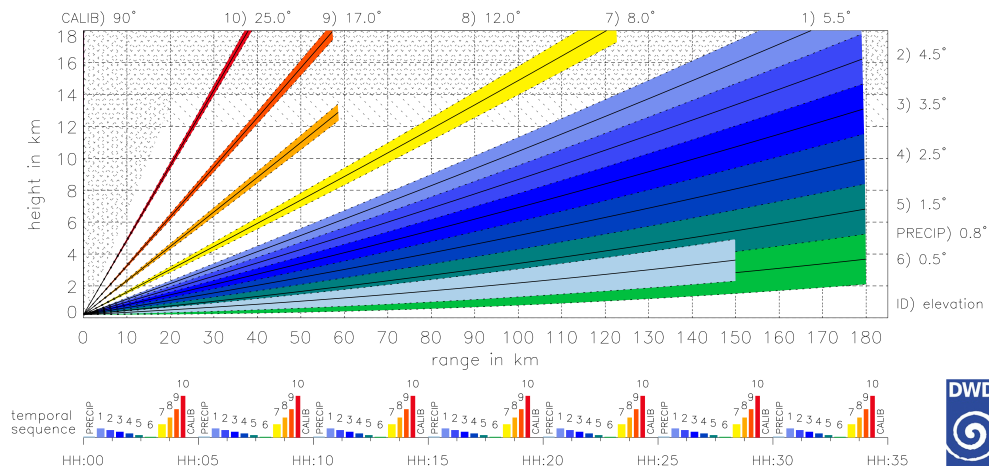


Figure 2. The DWD radar scan strategy since 2012 with its 10 volume scans and 1 precipitation scan.

“undefined” is unfortunately prone to errors. For this study we only included data with reports resulting in hail damage. For each date with hail damage information concerning the postal code, the damage expense, the number of damages, insurance expense and the number of insurance contracts in each postal code is provided. From April to September of 2013 to 2022 there are 526 444 insurance claims for different postal codes and days of hail. All in all, from 1830 possible days 1815 (99.18 %) are recorded as having at least one occurrence of hail damage in the area of Germany. This is because the damage cannot always be assigned to the precise day on which it occurred. The data is derived solely from postal code areas and may therefore not provide a complete picture of hail events. This limitation is why we chose to leave spatial analysis out of our examination of insurance data. By focusing primarily on larger hail events, we may inadvertently overlook occurrences of smaller hail, which are equally significant. So we focus on the temporal analysis of hail occurrences of insurance data.

3 Methods

This study focuses on two different radar-derived proxies to detect hail size: Vertically Integrated Ice (VII) and Maximum Expected Size of Hail (MESH). The first step as well for VII (Sec. 3.1) as for MESH (Sec. 3.2) is to collect the 11 radar elevation scans that will be used to construct a 3D data cube of reflectivity measurements, a composite in three dimensions. The geometric height of different temperature levels is derived from vertical temperature profiles of ICON-D2 (Icosahedral Nonhydrostatic) model (Reinert et al., 2020) and combined with the 3D data cube. For both algorithms, a minimum threshold of 7.5 mm is used to discriminate between hail and no hail.

3.1 VII

The Vertically Integrated Ice (VII) is a measure of the frozen water content in a vertical column. At DWD it is expressed in water equivalent and, therefore, differs from the definition established in the literature (Gauthier et al., 2006; Mosier et al., 2011). The height of the temperature with -10 °C H_{-10} is approximated by the height of the melting layer H_0 with a constant height offset. VII is calculated from the radar reflectivity Z by:

$$VII = \int_{H_{-10}}^{H_{-\infty}} 3.44 \cdot 10^{-6} Z^{\frac{4}{7}} dH \quad (1)$$

During the internal evaluation process of the VII product, forecasters proposed a linear relationship between observed hail size and VII: $VII_hailsize[mm] = VII \cdot 0.75$ (Böhme et al., 2017).

3.2 MESH

With the 3D data cube of reflectivities, it is possible to calculate the Severe Hail Index (SHI). The SHI is calculated by transforming reflectivity data (Z) between $Z_L = 40$ dBZ and $Z_U = 50$ dBZ ($W(Z)$) into hail kinetic energy flux (\dot{E}), applying a temperature weighting function ($W_T(H)$), and vertically integrating this value from the storm top to the radar level (Witt et al., 1998). The heights for the melting layer (H_0) and for a temperature of -20 °C (H_{-20}) are derived by ICON-D2.

$$W(Z) = \begin{cases} 0 & \text{for } Z \leq Z_L \\ \frac{Z-Z_L}{Z_U-Z_L} & \text{for } Z_L < Z < Z_U \\ 1 & \text{for } Z \geq Z_U \end{cases} \quad W_T(H) = \begin{cases} 0 & \text{for } H \leq H_0 \\ \frac{H-H_0}{H_{-20}-H_0} & \text{for } H_0 < H < H_{-20} \\ 1 & \text{for } H \geq H_{-20} \end{cases}$$

$$\dot{E} = 5 \cdot 10^{-6} \cdot 10^{0.084Z} W(Z) \quad \text{SHI} = 0.1 \int_{H_0}^{H_T} W_T(H) \dot{E} dH$$

From that we can deduce the Maximum Expected Size of Hail (MESH). First, MESH was derived by Witt et al. (1998). They used 147 hail observations for their derivation of SHI to MESH. As the intention of MESH is to anticipate the maximum possible hail diameter, the resulting value should be higher than 75 % of the observations. This leads to:

$$160 \quad \text{MESH[mm]} = 2.54 \cdot \text{SHI}^{0.5} \quad (2)$$

Murillo and Homeyer (2019) revised the approach and used 5897 observations to fit the power law. The resulting new power laws, one again with the MESH values higher than 75 % of the observations and one higher than 95 %:

$$\text{MESH[mm]}_{75} = 15.096 \cdot \text{SHI}^{0.206} \quad (3)$$

$$\text{MESH[mm]}_{95} = 22.157 \cdot \text{SHI}^{0.212} \quad (4)$$

165 Both fittings were made with S-band radars in the US. As we can make use of a great amount of observation data, we have derived our own SHI–MESH relationships for the German C-band radar network.

With the WarnWetter app we also have the opportunity to derive a power law for our region of interest. We must take into account, that the observations made via the WarnWetter app are given in categories. Therefore, we have selected the reference values from the category (see Sec. 2.1) e.g. a report from the category hail of 2 cm was assumed as an observation of a hailstone
170 with a diameter of 2 cm although it might be slightly smaller or larger. For the category "under 1 cm" a value of 0.5 cm and for "above 7 cm" a value of 7 cm were defined as reference. We took the highest SHI in a 5 km radius around the observation and in the last 15 minutes before the observation took place, as the report should be done after the hail reached the ground. Only data from April to September of the year 2022 and 2023 was used and SHI–observation pairs where the SHI was higher than 10. Our fittings for the larger hail sizes may not be optimal due to the lack of data. We had only 36 observations for 7cm, as
175 they are prone to errors and varied a lot in their SHI values, we left them out in the fitting. In total we had 2403 samples for 0.5 cm, 4232 samples for 1 cm, 1979 samples for 2 cm, 750 samples for 3 cm and 192 samples for 5cm. With that we receive the power laws out of 9556 observations:

$$\text{MESH[mm]}_{75} = 0.4607 \cdot \text{SHI}^{0.8665} \quad (5)$$

$$\text{MESH[mm]}_{95} = 0.9216 \cdot \text{SHI}^{0.9739} \quad (6)$$

$$180 \quad \text{MESH[mm]}_{\text{mean}} = 0.0071 \cdot \text{SHI}^{1.4877} \quad (7)$$

Figure 3 depicts the relations of SHI to reported hail sizes. It is important to note that the fitting to the power law is very sensitive.

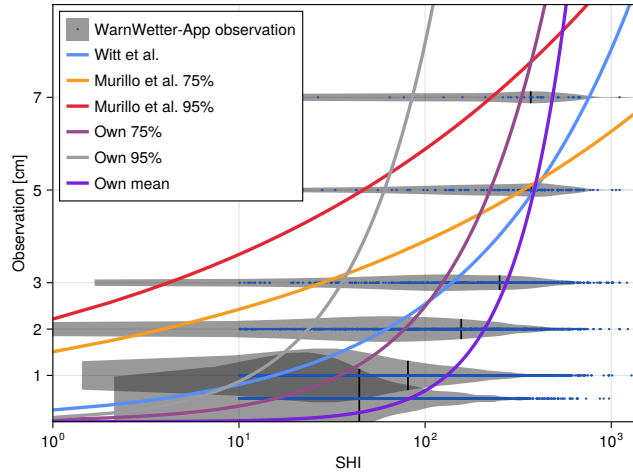


Figure 3. Comparison of all power laws of SHI (colored lines) to observation values (blue dots) in a violin plot visualizing the amount of observations (shaded area) including its median SHI (black vertical bar) of the data from the German WarnWetter app for the years 2022 and 2023.

4 Results

In the following, we present the results for hail observations in Germany, focusing on three key areas. First, we examine the human observed data, highlighting its quality and characteristics. Next, we analyze hail sizes and occurrences as detected by C-band weather radars, comparing the findings of two different algorithms with human observed data to assess their quality. Finally, we explore the economic impact of hail events through insurance data and show how hail events can lead to significant financial losses in the region.

4.1 Human observed data

In this section, we examine various sources of human observed data. We first assess the quality of crowdsourced data through a survey. This study used 3D printed hailstones to evaluate how precisely people estimate the size of hail. With these finding as context, we then present spatial and temporal patterns of human observed data across Germany.

4.2 Assessing the quality of human observed data

To develop and improve algorithms that identify hail events from radar observations, validation data is required. However, it is unclear whether user reports from the WarnWetter app are reliable enough to provide additional information for validation purposes. To answer this question, we conducted a brief study using 3D printed hailstones based on hail models (Mirkovic and Zrnic, 2023) (see Fig. 4).

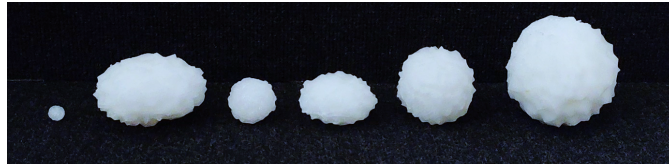


Figure 4. Six examples of 3D printed hailstones in different sizes and forms. From left to right: round 0.5 cm, oval 7 cm, round 2 cm, oval 5 cm, round 5 cm, round 7 cm

In total we had 12 hailstone samples in use, 6 round and 6 oval ones (diameter 2:1) with sizes of the maximum dimension of 0.5 cm, 1 cm, 2 cm, 3 cm, 5 cm and 7 cm. In the study we asked questions relating to 9 of those hail stones. In total we asked 149 participants (76 male, 68 female) with an age distribution found in Tab. 1. In Tab. 2 the number of interviews for the different sizes and the form of the hailstones are listed. After the participants accepted the data processing, they were asked to estimate

Age range	Participants
under 20	23
20–40	72
40–60	30
above 60	21
no answer	3

Table 1. The number of people asked in the different age groups categorized by age.

Size	Form	Number of interviews
3 cm	round	15
3 cm	oval	23
7 cm	oval	7
1 cm	round	11
5 cm	oval	14
2 cm	oval	11
7 cm	round	14
1 cm	oval	23
5 cm	round	31

Table 2. The number of interviews for each hailstone.

the diameter of a 2€ coin to obtain a control value for their ability to estimate sizes, independently of a hailstone. Afterwards, they were asked to estimate the size of the presented hailstone. The survey included two separate values. In the first phase, participants were asked to answer freely. In the second phase, they were given options for their answers. The options were the

205 same as in the reporting process of the WarnWetter app.

Hagelkorngröße (hail size)

- Unter 1 cm (Linse) (under 1 cm lentil)
- 1 cm (Erbse) (1 cm pea)
- 2 cm (10 Cent Münze) (2 cm 10 cent coin)
- 210 – 3 cm (Kronkorken) (3 cm crown cork)
- 5 cm (Golfball) (5 cm golfball)
- Über 7 cm (Tennisball) (above 7 cm tennisball)

In addition, demographic data was gathered for statistical evaluation.

The true value of the diameter of a 2€ coin is 2.575 cm. The estimated mean diameter of all survey participants is $M =$
215 2.538 cm, with a minimum of 1 cm and a maximum of 6 cm. We were interested in determining whether there is a discrepancy
among age groups due to differing degrees of experience with the digital world or its attendant technologies. The distribution
of answers for the different ranges of age can be found in Fig. 5. Most of the age groups underestimated the size of the coin,
only the 20–40 year olds overestimated the size in the mean, but in the median they were very good with 2.5 cm. The best
mean achieved the under 20 year olds with $M = 2.508$ cm, but they had as well as the 20–40 year olds some outliers with 5–6
220 cm and the median is too low.

Figure 6 depicts that with the categories as options, the participants had chosen the right category in most of the times (75.17
%). Nevertheless, in case of wrong categories mostly smaller ones were chosen (18.79 %). There is no difference for round and
oval hailstones visible. Figure 6 also shows the free estimation of hail stone size in cm as a kernel density estimation. Without
the option to choose a category, the distribution of answers is much broader, still with a median that is close to the right size.
225 The distributions are almost symmetrical, with a median which tends to be too small. The deviation to the true value stays
similar through all sizes.

At the end, we compared the results of the initial estimation question about the size of the 2€ coin with the results of the freely
given answers for the hailstones. Figure 7 clearly shows that there is no clear linear relationship between those two answers.
This may be due to the fact, that the hailstone was presented and could be touched. Most of the participants needed to imagine
230 the size of a 2€ coin.

In a nutshell, we can say that the mean of the estimated sizes is quite good and close to the real value, but individual estimations
can be quite inaccurate. It seems that estimating the size of an object of imagination, like the 2€ coin in our survey, is not
directly comparable to an object that is visible. Most of the answers to the categorical options were right, but there are also
some wrong answers. As we have a low spatial density of observations in the WarnWetter app most of the time, we need to keep
235 in mind, that there might be wrong values due to bad estimation abilities. If the estimation of the size is off, it is likely to be

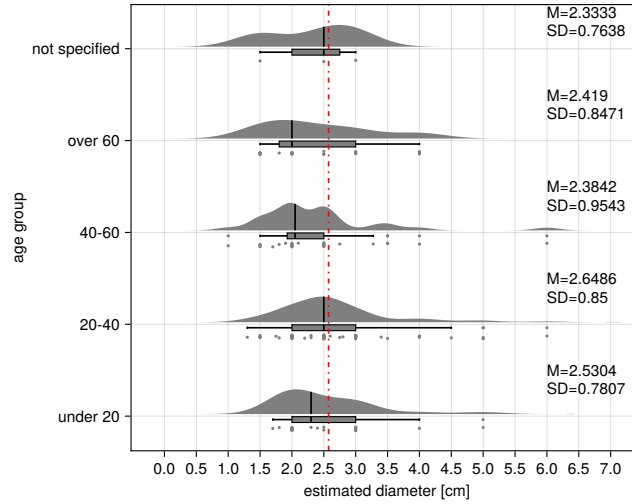


Figure 5. The distribution with its median of answers (black vertical bar) for the question *How large is a 2 € coin?* in the different age groups. The correct answer is shown as red dashed line. The mean and standard deviation for each group are presented in the figure on the right. The answers are shown in three different visualizations: The upper one: a kernel density estimation for all answers in the age group showing the different distributions of answers; the middle one: a box plot showing the quartiles and outliers; the last one: the answers as single dots showing all single values.

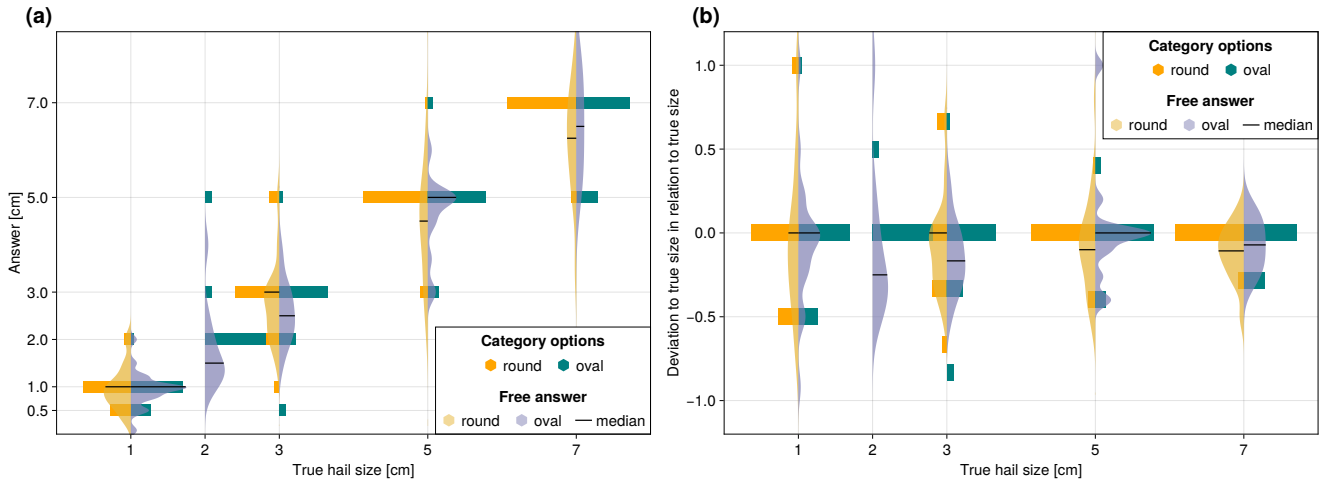


Figure 6. (a): The distribution of answers to the category options for estimating the size of the presented hailstone as bars and the free answers as kernel density estimation with its median. (b): The deviation to the true hail size in relation to the true hail size.

underestimated. The bias remains constant irrespective of hail size; however, the standard deviation undergoes a reduction for larger hail sizes. Giving the categories seemed useful, as only for small hail sizes, the number of wrong categories is noticeable.

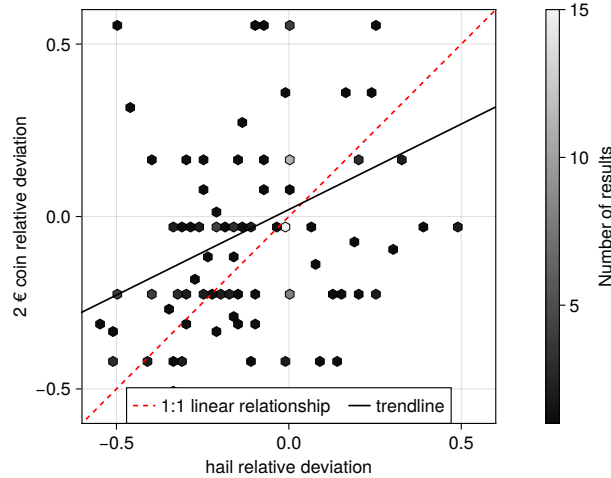


Figure 7. The comparison of deviations from the estimation of the size of a 2€ coin and the freely given answers to the hailstone size estimation.

4.3 Analysis of crowdsourced data in Germany

Based on crowdsourced data from ESWD, WarnWetter app and station observations we will address the questions of diurnal
 240 and annual cycles and hotspots of hail in Germany. In Fig. 8(a) the diurnal cycle of hail reports is depicted. For this analysis the station observations were excluded due to missing information concerning the time of the hail event.

The number of hail observations clearly shows a diurnal cycle, as the reports are very close to be normally distributed around
 15 UTC (17 CEST), with a standard deviation of about 3 hours. Reports of night time (23 UTC–8 UTC, 1 CEST–10 CEST)
 hail events are rare. There are also two months in which there is a higher probability of hail being observed, namely May and
 245 June (see Fig. 8(b)). Beyond the convective season the number of reports is negligible with the exception of March 2021 and February 2022. All in all, there are much more reports of the WarnWetter app than from the ESWD, visible through the higher numbers since 2021. Figure 9 depicts the reported sizes in the ESWD and the WarnWetter app. Small hail is more prominently occurring from February to September, medium hail occurs mainly in June, but also in May, July and August. In Germany only a few reports of hail that exceeded 5 cm were recorded in the last 23 years. Large to giant hail is most likely to occur from May
 250 to August.

The distribution of hail reports in Germany is displayed in Fig. 10(a) in a h3 grid of level 6 (Uber Technologies Inc., 2018). There are some hotspots visible in the south of Bavaria (close to Munich), in the middle of Baden–Wuerttemberg (close to Stuttgart), North Rhine–Westphalia in the Ruhr valley, Hessia in the Rhine–Main region and Berlin. In the north of Germany there are only a few hail reports. All areas with hail hotspots have a high population (see Fig. 10(b)). To examine whether
 255 the observations underlay an urban reporting bias, Fig. 10(c) shows the number of observations in a cell, normalized to the population. No such hotspots are visible any longer, only the Pre–Alps have a slightly higher number of observations than the

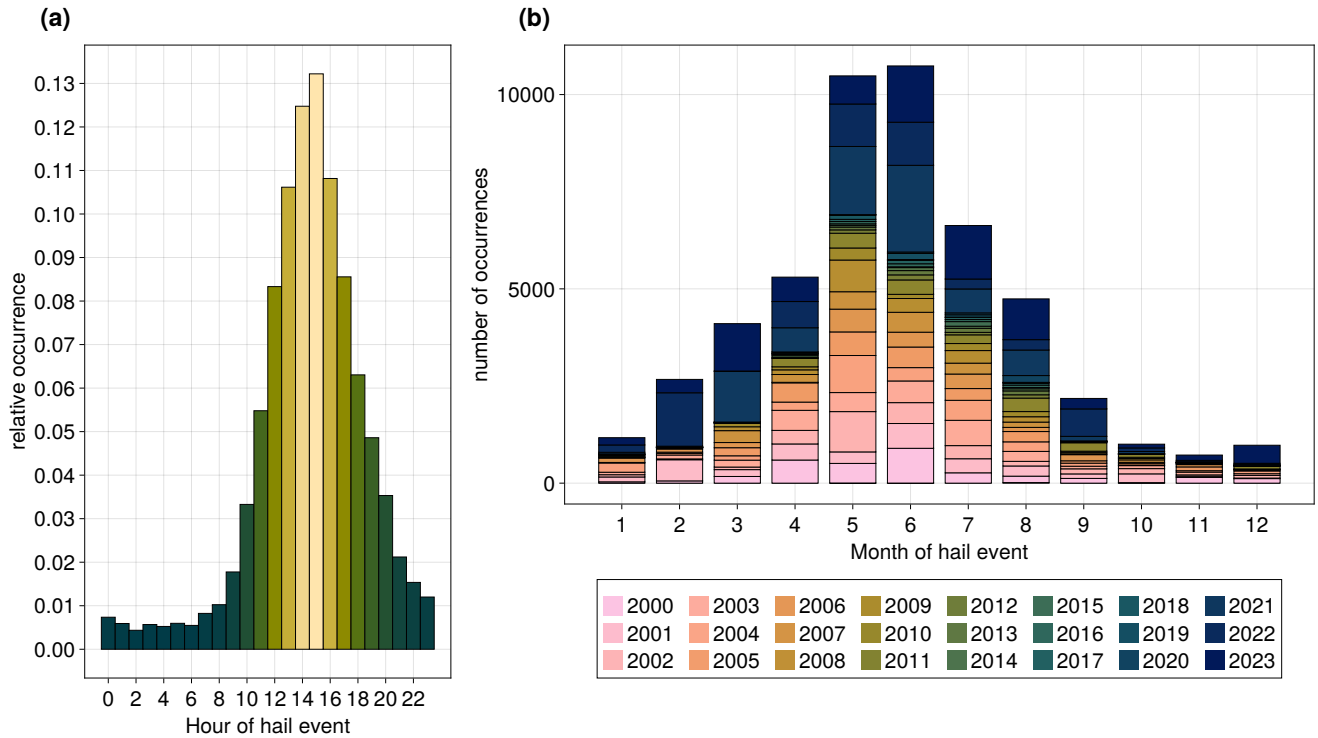


Figure 8. Hail observations in its (a) diurnal cycle based on data from ESWD (3769) and WarnWetter app (21 231) and (b) annual cycle based on data from station observations (25 719), ESWD (3769) and WarnWetter app (21 231).

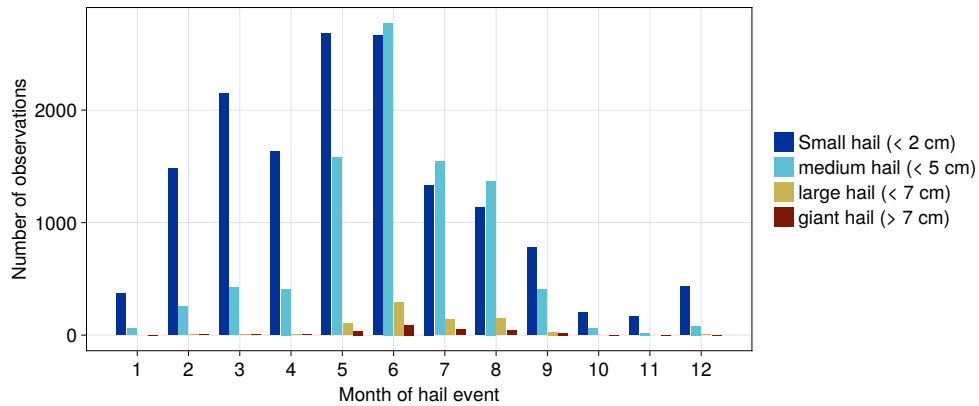


Figure 9. Distribution of hail sizes of observations in Germany from the ESWD and the WarnWetter app.

rest of Germany. Some cells are more noticeable because of station observations that have been in one place for a long time

and therefore reported hail for each day if apparent. In conclusion, the absence of hotspots in the normalized Fig. 10(c) clearly emphasizes the existence of an urban reporting bias, as there is no longer a visible difference in hail occurrence over Germany.

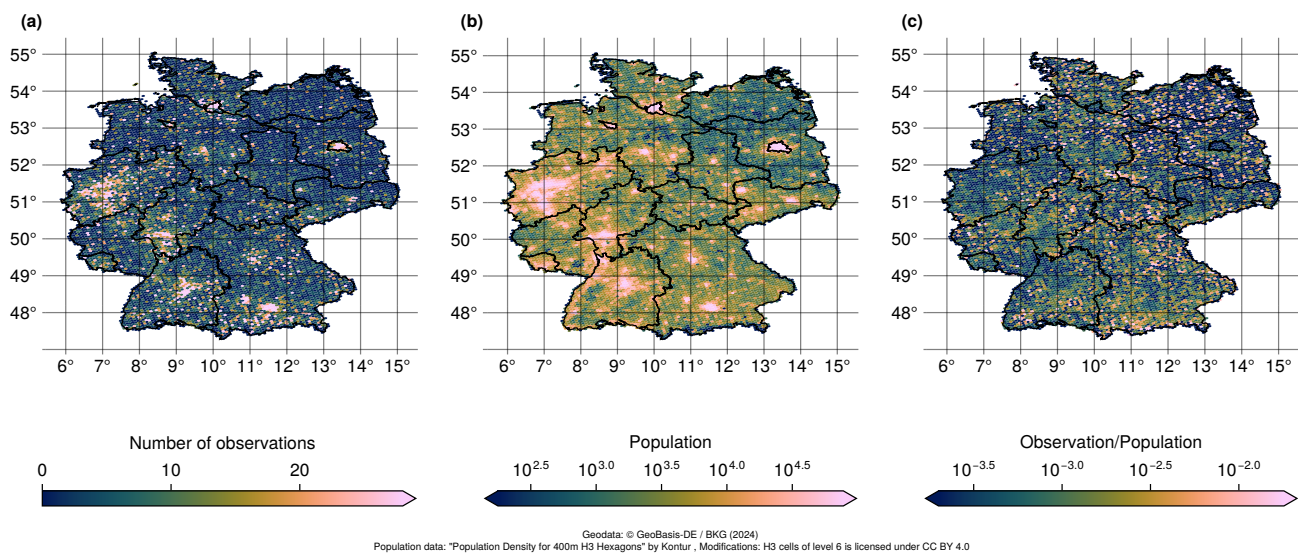


Figure 10. (a) Number of crowd observations in Germany 2001–2023 based on data from station observations, ESWD and WarnWetter-App. (b) Population in Germany (c) Normalized number of observations to the population

In this section, we use a case study to analyze hail sizes derived from C-band weather radars using two methods: MESH and VII. We then compare these results with human observations. Based on our results, we focus on VII to describe hail characteristics in terms of size and occurrence across Germany.

4.5 Comparison of VII and MESH

265 For the comparison of MESH, VII and crowd data, we use the relationship of SHI to MESH we developed for the German C-band radar network of 75% (Eq. 5). We compare the performance of MESH to the data of the reported sizes in the WarnWetter app for a case study of a hail event from 15 August 2021 (see Fig. 11). Further on, we have a look at differences between the resulting MESH sizes and the sizes retrieved by VII (compare Fig. 11 (a) with Fig. 11 (b)). In instances where the value of MESH/VII exceeds 7.5 mm, the presence of hail is assumed. Consequently, it is highly improbable that we can provide
270 coverage for hail reports categorized as "smaller than 1 cm".

Generally, we see that the hail track is matched quite well for MESH and VII in comparison to the crowd data. The MESH hail size is larger than the VII hail size. The MESH track shows more areas with small hail sizes. Most of the crowd data are reported within those two tracks, only a few reports of small hail are located outside the tracks. MESH overestimates the sizes clearly. VII has similar magnitudes of hail size compared to the observations, and the locations also fit quite well. To
275 show a more complete picture for different MESH formulas and VII compared to the observations, we have validated all of those algorithms with hail days in 2024 that were not used for the MESH fitting (see Tab. A1). From that we can say that VII performs best for hail sizes up to 3 cm. The MESH formula that uses the mean instead of the 75 % percentile is also very good. For larger hail sizes there were only a few observations, but for them, the 75 % formulas of MESH (as well the one of Murillo and Homeyer (2019) as our own fit) outperform VII. The result is not unexpected, because MESH is fitted so that 75%,
280 95% respectively, of the values is lower so that we can be very sure that the resulting hail size is the maximum expected. VII does not try to find the maximum value of hail. For most of the observations (75 %) the MESH value is too large, so in total MESH does not perform as well as VII, especially for smaller hail sizes. For the larger observation values MESH performs better because of the assumption for fitting the formula. Both VII and MESH, therefore, take different aspects of hail size into account. We have chosen VII for a larger analysis over the period 2018–2023, as it fits better for most of the values.

285 4.6 Multi annual analysis of Vertical Integrated Ice (VII) in Germany

The study covers a relatively short period of 6 years from 2018–2023, but nevertheless it can give great insides to the hail distribution over Germany. First we have a look at the total hail days in the period under review. In Fig. 12 the mean number of hail days from 2018–2023 based on VII is shown.

The occurrence of hail shows a gradient from north to south with a maximum in the alpine foothills of Bavaria. However,
290 according to the VII approach, 80.6 % of Germany within a 1x1 kmš area is hit by hail at least once in those 6 years. The mean number of hail occurrences per year is about 0.33, this means approximately 2 hail events in the analyzed period. The

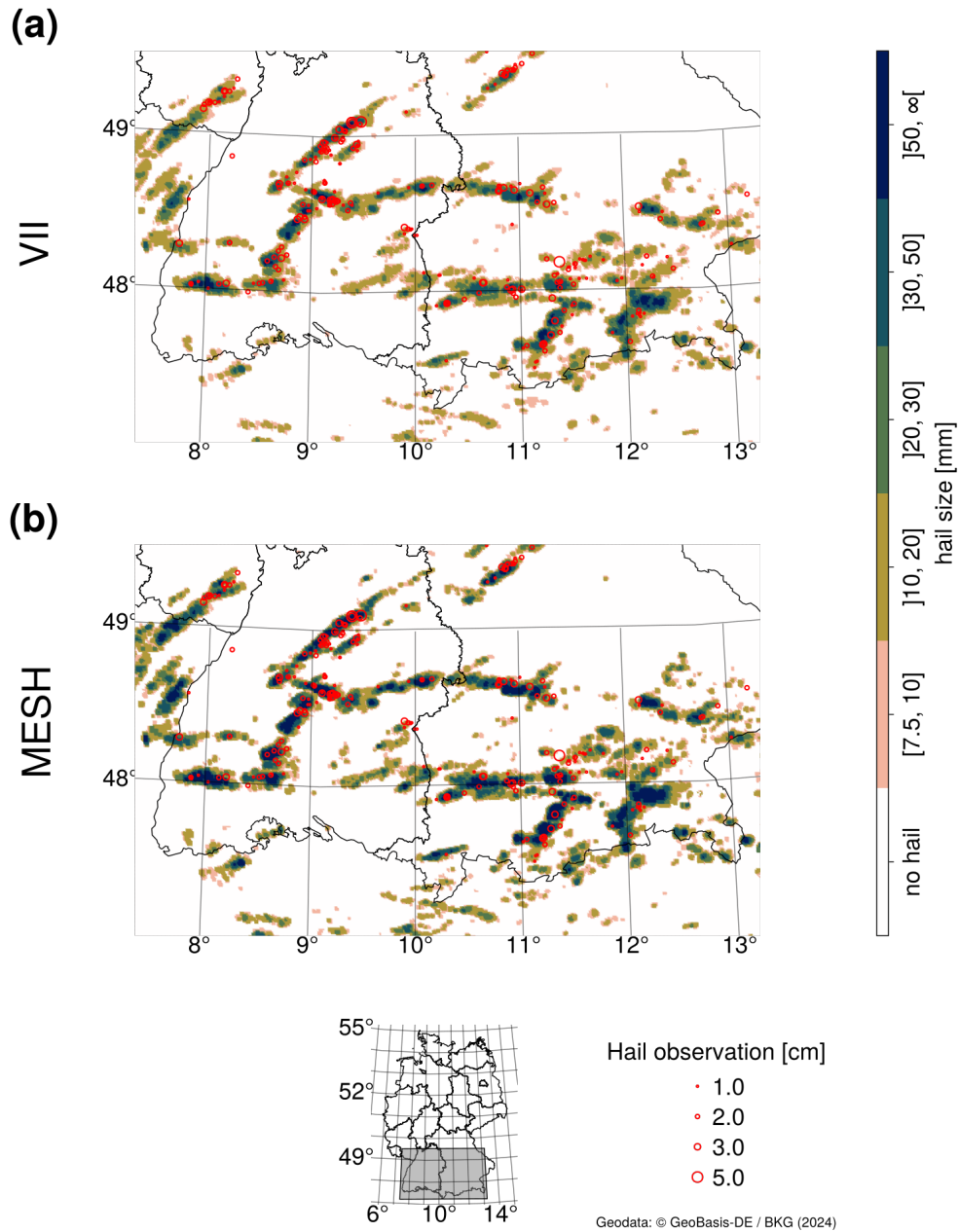


Figure 11. (a) VII with Crowd data from 15.08.2021 zoomed into southern Germany. (b) MESH with crowd data from 15.08.2021 zoomed into southern Germany.

maximum number of hail days for one gridcell is 19 days in the timeperiod. The largest amount of hail days can be found in the German low mountain ranges in the most southern part. Although, Fig. 12 shows that hail is possible everywhere in Germany,

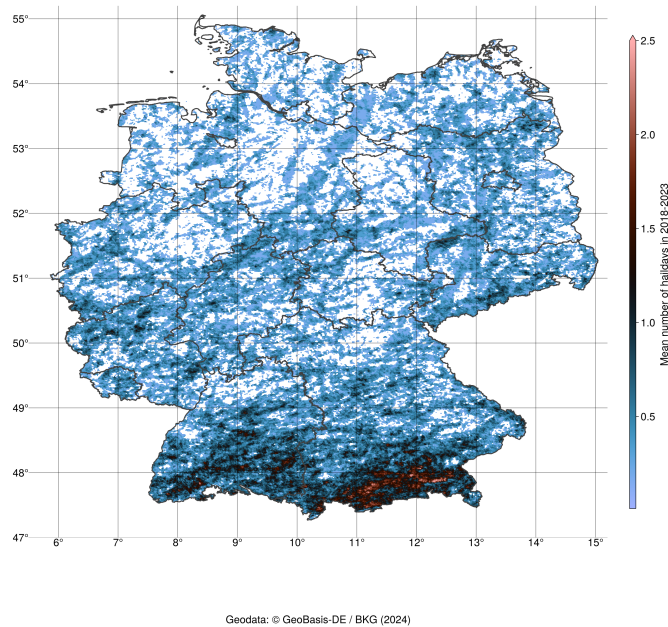


Figure 12. Mean number of hail days in a year based on VII from 2018–2023

hail occurrence and hail size strongly depend on single storm tracks. The number of hail days in 2019 in Fig. 13(a) shows hot spots in the eastern part of Germany, contrary to 2021, in Fig. 13(b), where there are hot spots in the Pre-Alps. In 2019 only 25 kmš, in 2021 almost 900 kmš had more than 4 hail days in Germany.

Also the maximum hail size in each year is highly influenced by single storms (see Fig. 14). On average the maximum hail size is about 1.5–3cm depending on each year. Single storms producing clearly visible hail tracks (see Fig. 14(a)) which also lead to larger hail sizes. One of the largest hail storms in the recent years can also be seen in Fig. 14(b). The hotspot of maximum hail sizes is situated directly over Kassel (mid of Germany) with hail larger than 7 cm. The area with extreme hail has a large track and a large width.

The maximum hail size over 2018–2023 is shown in Fig. 15. There are only very few hail days with hailstones larger than 5 cm. Over southern Bavaria, individual cell tracks are discernible, suggesting that the most severe hail events are caused by isolated extreme convective cells. Most of the detected hail sizes are smaller than 2 cm. The occurrence of hail using VII shows a clear annual cycle (see Fig. 16) which is in accordance to the results with crowdsourcing data (Sec. 4.1). From April to June (Fig. 16(a)–(c)) the number of hail days increases, with numbers subsequently decreasing again afterwards till September (Fig. 16(d)–(f)). Before April and after September, VII cannot detect any reasonable amounts of hail. A similar annual cycle can be observed for the maximum hail size (see Fig. 17). In April (Fig. 17(a)) there are some hailstorms, but with only small sizes. In

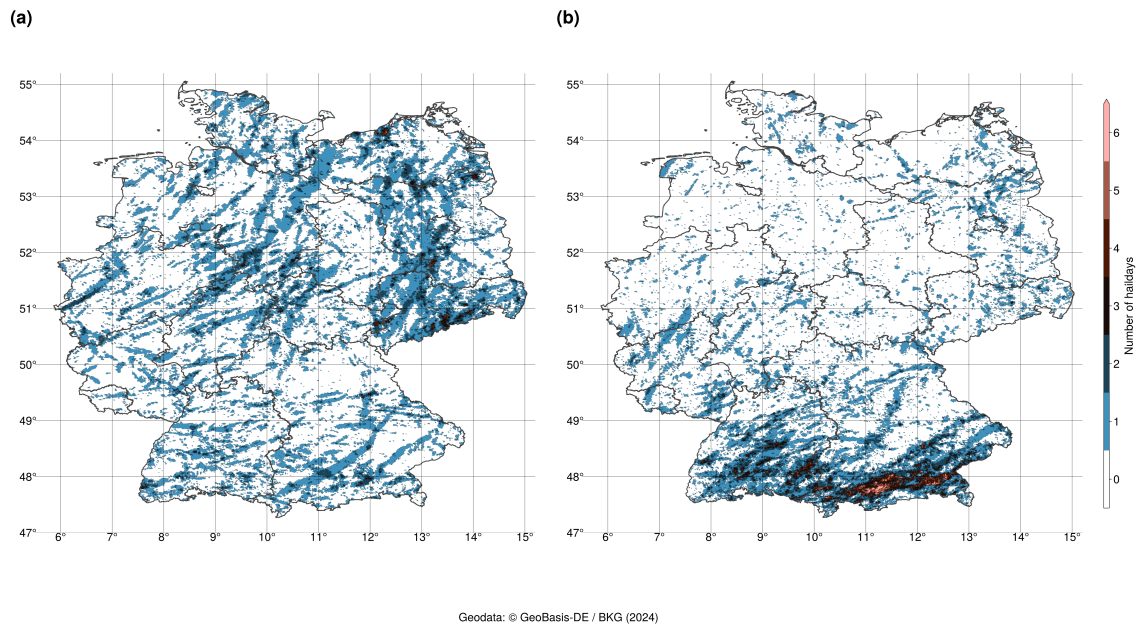


Figure 13. Two example number of the number of hail days basaed on VII with very distinct hotspots (a): in 2019 (b): in 2021

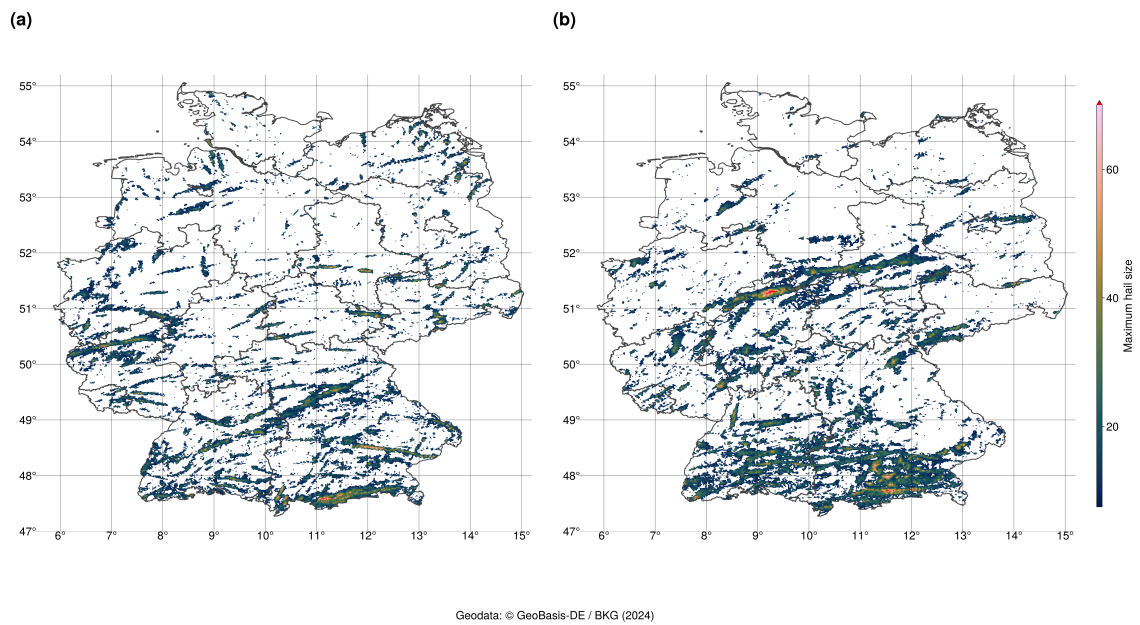


Figure 14. Two examples of the maximum hail size based on VII (a): in 2022 and (b): in 2023

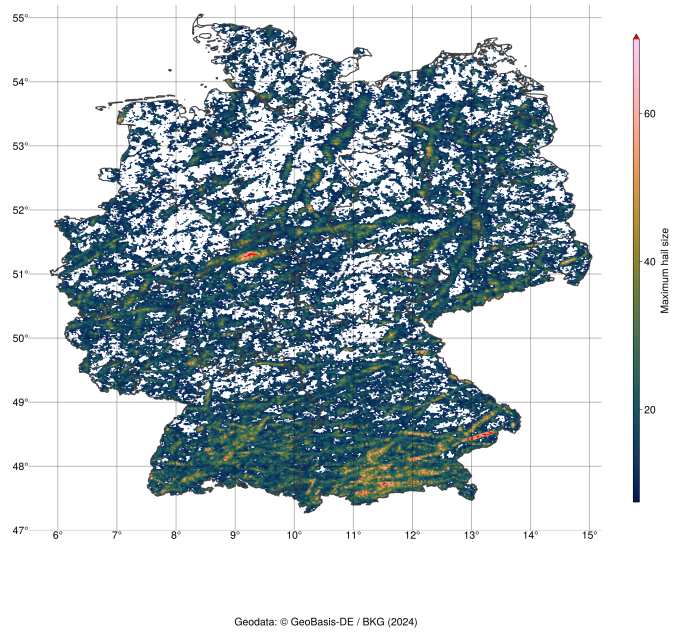


Figure 15. The maximum hail size based on VII for each pixel over 2018–2023.

May (Fig. 17(b)) the sizes are getting larger, until finally peaking in June (Fig. 17(c)). In the Pre-Alps large hail also occurred
 310 in August (Fig. 17(e)) during the investigated period.

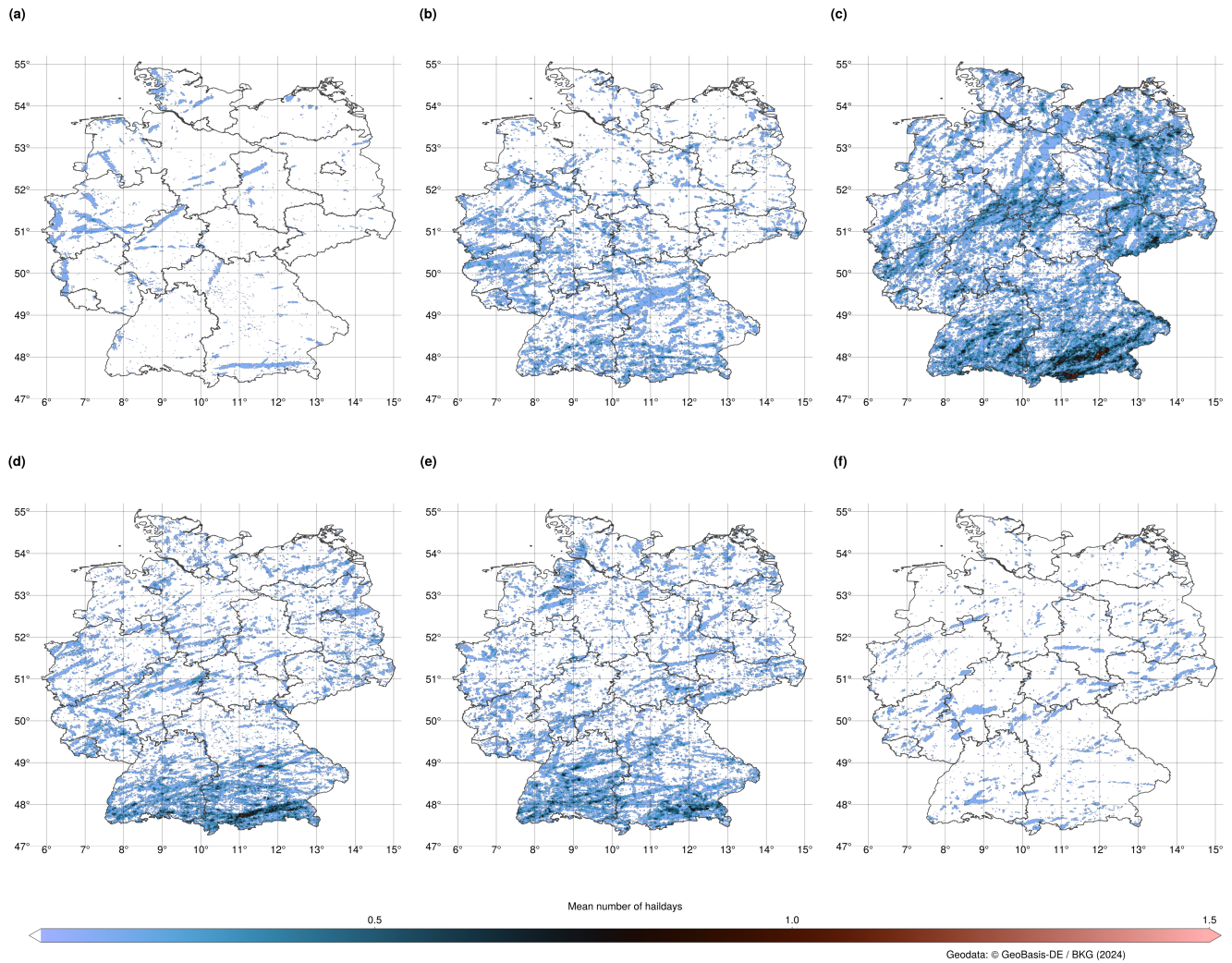


Figure 16. The annual cycle of hail days from 2018 to 2023 in Germany based on VII from (a): April (b): May (c): June (d): July (e): August (f): September

4.7 Insurance data

The analysis in Fig. 18 depicts that June is the month with the most damage caused by hail with a mean of 33 972 damage reports. In July, a similar mean number of damages is reported in terms of the number of damage reports, with a mean of 29 492. The hailstorm that occurred in July 2013 had a significant impact on the mean number of damage reports. If 2013 is left out of this analysis, the mean drops to only approximately 15 002 damage reports. The number of reports on damage in April ($M = 1509$) and September ($M = 1228$) is relatively low, while in May ($M = 9230$) and August ($M = 11526$), the number of reports is in the midfield. The loss expenses show a very similar picture to the number of damage reports. It is quite interesting

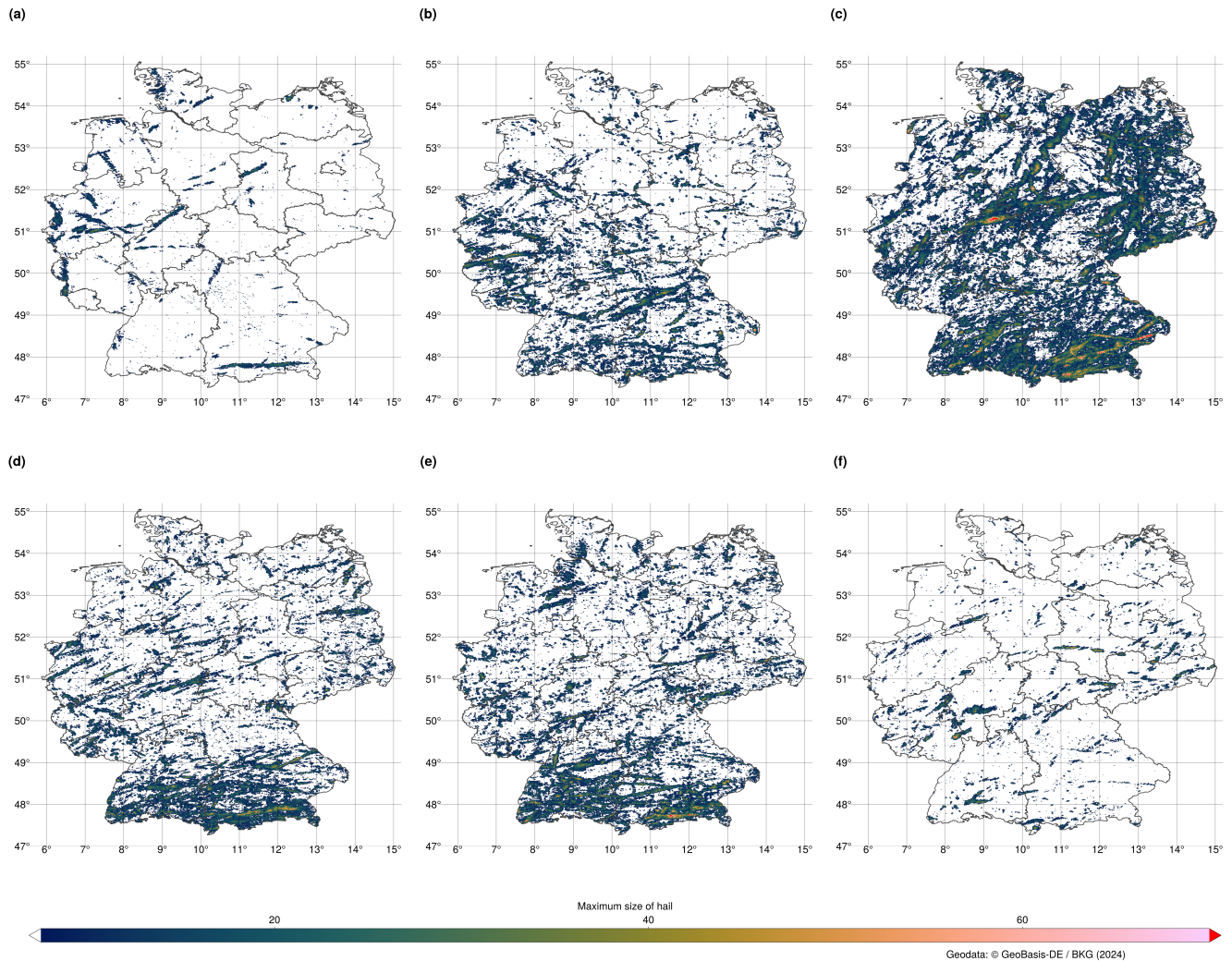


Figure 17. The annual cycle of hail sizes from 2018 to 2023 in Germany based on VII from (a): April (b): May (c): June (d): July (e): August (f): September

that in 2022 the loss expenses in May (100.43 Mio €) and September (21.2 Mio €) are much higher than in the years before (May: $M=24.53$ Mio €; September: $M=3.18$ Mio €). In June, July and August 2022 the loss expenses are on a similar level or smaller.

We can compare the number of damage reports, which is equally true for the loss expenses, to the number of observations in total (see Fig. 8) as well as to the distribution of hail sizes (see Fig. 9). Both, number of damage reports and number of hail observations (Fig. 8), show a clear annual cycle with a peak in the summer months, moderate numbers of reports and observations in spring and autumn and almost no hail events in winter. The maximum of damage reports, however, is in June and July and, therefore, shifted to later in the year compared to the observations with a maximum in May and June. This

might be due to the hail size: Figure 9 indicates that small hail dominates in winter, spring and autumn, while medium sized hail dominates in the summer months probably leading to enhanced damage. Large and giant hail with the highest damage potential almost exclusively occur from May to August. In case of leaving out the extreme hail event in July 2013 in the damage reports, their maximum is in June as well as the maximum for medium to giant hail observations.

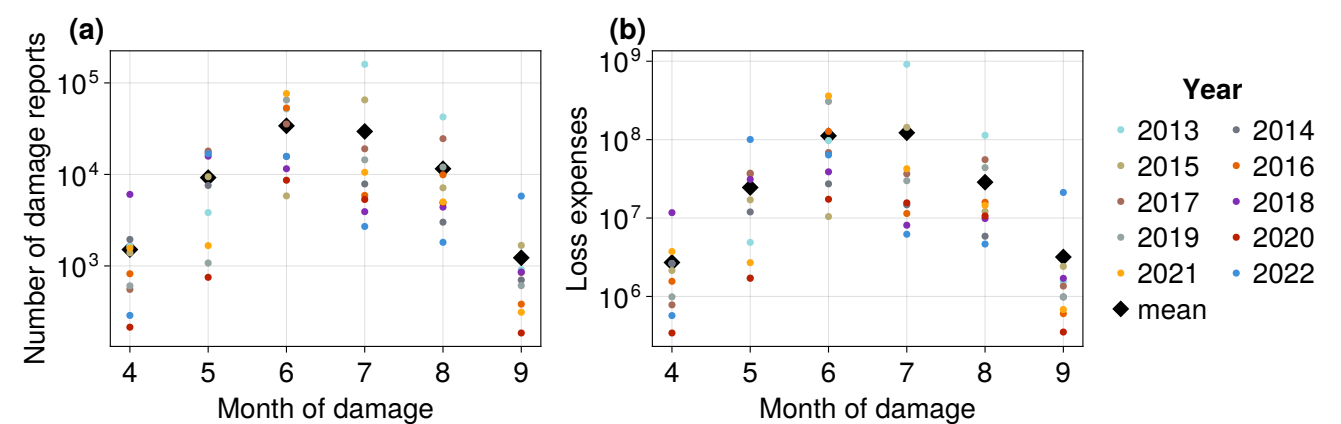


Figure 18. Insurance data for the summer months each year 2013–2022. (a) Number of damage reports. (b) Sum of loss expenses.

330 5 Summary and future work

As hail is a weather phenomena which is hard to observe and measure, only a few studies about spatial and temporal patterns for hail in Germany exist. In this study we investigated hail statistics for Germany derived from human observed data and C-band weather radar data using the methods vertically integrated ice (VII) and maximum estimated size of hail (MESH). We used crowdsourced data by the WarnWetter app operated by the DWD, manned weather stations and ESWD data to analyze
335 mainly temporal patterns of hail occurrence. With the benefit of spatial coverage, radar data were used to overcome the lack of spatial information in human observed data. Insurance data give us a hint on the destructiveness of hail in the measure of loss expenses.

In what follows, we attempt to answer the questions posed in the introduction. Our first focus is on the question “Can we rely on human observed hail data in their size estimation?”. The use of human observation data is challenging for the use of hail size
340 estimation. The location, date and time may be more reliable than the actual size of the hail estimate. In our study, we found that the mean of many observations is usually very good, but individual observations can be misleading. If the size is wrongly estimated, it is more probable to be underestimated. Giving a category with a known object for reference in mobile phone applications brings a benefit over freely given values. Further on, the number of observations underlays the urban reporting bias, as more observations are reported in areas with higher population. Therefore, human observations should be treated with
345 caution, but can still give us a good first idea of the hail event.

To overcome the problem of urban reporting bias, radar data can be used, but “Are the radar based algorithms VII and MESH suitable for determining hail (size) climatologies for Germany?” Even despite the use of the own developed relationship of SHI and hail size, MESH clearly overestimates the hail size in comparison with crowdsourced data. VII gives similar hail sizes as human observed data in our case study. Therefore, we used VII for showing maximum hail sizes and hail occurrences in Germany for our study period of 2018–2023.

For answering the question if hail events in Germany are rare or frequent natural hazards, we can combine results of radar data and human observed data. Unfortunately, there is no clear answer to this question because the frequency of hail is quite variable in Germany. Large to giant hail is very rare in Germany. The south of Germany has a higher chance to be hit by large hail and is typically hit more frequently by hail storms than the north. Nevertheless, also large hail events are possible all over Germany like the hailstorm in the middle of Germany 2023 has shown. Púčik et al. (2019) and Kaltenböck et al. (2009) used the ESWD data to analyze the diurnal cycle of hail in Europe. Their findings that the diurnal peak of hail occurrence is about 15–16 UTC can be confirmed also with the longer timeseries of this study for Germany. It must be noticed that crowdsourced data are likely biased in terms of diurnal cycle with an underrepresentation during night. Púčik et al. (2019) depicted a similar annual cycle pattern for southern Europe (regions south of 46°N latitude) to the annual cycle found by this study. For regions north of 46°N they found more activity in July. With the VII derived from radar data we clearly see June as the month with the most hail days for whole Germany.

For crowdsourced data the analysis showed many reports in the highly populated Ruhr and Rhine–Main area and in the larger cities like Berlin and Munich (urban reporting bias). The hotspot close to Stuttgart (south–west Germany) that was found previously (Puskeiler et al., 2016) can be seen in the VII data.

With the use of radar based algorithms, we can produce a picture of hail over the whole of Germany. We can confirm the overestimation of MESH, which Brook et al. (2024) has overcome with an empirical correction. We have chosen VII for the multi year analysis, as it fits better the crowd data in our case study in terms of hail size. The case study shows that the hail tracks of MESH and VII fit quite well to the observations.

Only through observation data it is currently not possible to calculate any trends in hail occurrence, due to a varying number of observers over the years. The WarnWetter app introduces much more active observers than we had before. The same is true for the ESWD data that increased in number of reports over time. With radar data we see years with a lot of hail, e.g. 2021, and years with few hail, e.g. 2020. Overall, the analyzed period of 6 years is not long enough to define a trend and was out of scope of this study. For trend analysis modelled data (Battaglioli et al., 2023; Wilhelm et al., 2024) might be a better fit as long as other consistent time series are too short.

A question for the future is to determine the most appropriate metric for determining the severity of hailstorms. Should the largest individual hailstone be used as the benchmark? Alternatively, could we consider an average diameter? What is the ground truth for this approach? An alternative approach would be to omit the exact hail sizes and identify the impact or damages directly (e.g. (Schmid et al., 2023)). If crowdsourced data is used, it is important to consider the potential biases that may affect the results. The position may be inaccurate, there may be a population bias, and there is a possibility that only large hail is being reported. Additionally, there is an estimation problem and a diurnal cycle for reporting. For future

work, it might be interesting to recalculate VII for earlier years to see if there are any patterns or trends in hail occurrence in Germany. Furthermore, the SHI–MESH relationship could be fitted to a longer time series of observed data. For the refitting the observations could be pooled to use only the mean of neighboring observations and to take only observations into account with neighboring observations available. A similar approach of refitting could be applied to the VII data to increase the performance even further. As we have some diverse data sources, artificial intelligence methods could be beneficial to combine all data sources and result in impacts for the population or hail probability.

Appendix A: Validation of MESH and VII with some case days

Observation size	Method for hail size estimation	MAD ^a	MSD ^b	RMSD ^c	Normalized RMSD ^d
All sizes (579 samples)	MESH ^e	38.258	2513.54	50.131	0.319
	MESH ^f	29.921	1014.456	31.851	0.507
	MESH ^g	22.347	1278.128	35.751	0.226
	VII	15.051	401.761	20.044	0.255
Smaller 1 cm (92 samples)	MESH ^e	25.677	1475.933	38.418	0.251
	MESH ^f	31.42	1155.119	33.987	0.544
	MESH ^g	12.805	711.918	26.682	0.176
	VII	12.999	370.384	19.245	0.255
1 cm (247 samples)	MESH ^e	39.414	2763.308	52.567	0.335
	MESH ^f	34.161	1263.741	35.549	0.565
	MESH ^g	22.831	1414.403	37.609	0.238
	VII	17.08	490.905	22.156	0.284
2 cm (153 samples)	MESH ^e	39.136	2431.463	49.31	0.336
	MESH ^f	27.546	813.61	28.524	0.461
	MESH ^g	22.535	1152.775	33.953	0.24
	VII	12.686	288.434	16.983	0.234
3 cm (73 samples)	MESH ^e	49.709	3290.305	57.361	0.375
	MESH ^f	22.78	565.842	23.787	0.381
	MESH ^g	31.159	1778.604	42.173	0.279
	VII	14.784	354.579	18.83	0.25
5 cm (13 samples)	MESH ^e	33.385	1890.514	43.48	0.284
	MESH ^f	7.713	219.103	14.802	0.237
	MESH ^g	28.595	1401.915	37.442	0.248
	VII	18.631	452.086	21.262	0.297
larger 7 cm (1 sample)	MESH ^e	3.228	10.419	3.228	-
	MESH ^f	17.829	317.882	17.829	-
	MESH ^g	27.282	744.293	27.282	-
	VII	37.406	1399.189	37.406	-

Table A1. Statistical analysis for different days with hail in 2024 for MESH fitted with our own data, MESH 75% by Murillo and Homeyer (2019) and VII compared to data from the WarnWetter app. For the algorithms the maximum value of the last 15 minutes before the observation with a radius of 5 km around the observation was taken.

^a Mean absolute deviation ^b Mean squared deviation ^c Root mean squared deviation ^d Normalized root mean squared deviation
^e MESH from own fitted 75% ^f MESH fitted by Murillo and Homeyer (2019) 75% ^g MESH from own fitted mean

. TW prepared the original draft of the manuscript, performed data analysis, including coding and plotting. MS implemented the algorithms. All authors have contributed to the manuscript and to the interpretation of the results.

390 . The authors declare that there are no competing interests.

. Thanks to the German Insurance Association for providing access to their data. The figures 3, 5–18 were produced with the Makie.jl ecosystem (Danisch and Krumbiegel, 2021).

References

- Naturgefahren in Deutschland, <https://www.dkkv.org/de/naturgefahren-in-deutschland>, 2021.
- 395 Naturgefahrenbilanz 2023: 4,9 Milliarden Euro Schäden durch Wetterextreme, <https://www.gdv.de/gdv/medien/medieninformationen/naturgefahrenbilanz-2023-4-9-milliarden-euro-schaeden-durch-wetterextreme--162854>, 2023.
- Ackermann, L., Soderholm, J., Protat, A., Whitley, R., Ye, L., and Ridder, N.: Radar and Environment-based Hail Damage Estimates using Machine Learning, *Atmospheric Measurement Techniques Discussions*, 2023, 1–24, 2023.
- Allen, J. T. and Tippett, M. K.: The characteristics of United States hail reports: 1955–2014, *E-Journal of Severe Storms Meteorology*, 10,
400 1–31, 2015.
- Aydin, K., Seliga, T., and Balaji, V.: Remote sensing of hail with a dual linear polarization radar, *Journal of Applied Meteorology and Climatology*, 25, 1475–1484, 1986.
- Battaglioli, F., Groenemeijer, P., Púčik, T., Taszarek, M., Ulbrich, U., and Rust, H.: Modeled Multidecadal Trends of Lightning and (Very) Large Hail in Europe and North America (1950–2021), *Journal of Applied Meteorology and Climatology*, 62, 1627–1653, 2023.
- 405 Brook, J. P., Soderholm, J. S., Protat, A., McGowan, H., and Warren, R. A.: A Radar-Based Hail Climatology of Australia, *Monthly Weather Review*, 2024.
- Brown, T. M., Pogorzelski, W. H., and Giammanco, I. M.: Evaluating hail damage using property insurance claims data, *Weather, Climate, and Society*, 7, 197–210, 2015.
- Böhme, T., Herold, C., and Schapper, S.: Poster: Use of new radar products for nowcasting of severe storms, in: *European Conference on*
410 *Severe Storms*, 2017.
- Danisch, S. and Krumbiegel, J.: Makie.jl: Flexible high-performance data visualization for Julia, *Journal of Open Source Software*, 6, 3349, <https://doi.org/10.21105/joss.03349>, 2021.
- Depue, T. K., Kennedy, P. C., and Rutledge, S. A.: Performance of the hail differential reflectivity (H DR) polarimetric radar hail indicator, *Journal of Applied Meteorology and Climatology*, 46, 1290 – 1301, 2007.
- 415 Dotzek, N., Groenemeijer, P., Feuerstein, B., and Holzer, A. M.: Overview of ESSL’s severe convective storms research using the European Severe Weather Database ESWD, *Atmospheric research*, 93, 575–586, 2009.
- Fluck, E., Kunz, M., Geissbuehler, P., and Ritz, S. P.: Radar-based assessment of hail frequency in Europe, *Natural Hazards and Earth System Sciences*, 21, 683–701, 2021.
- Foote, G. B., Krauss, T. W., and Makitov, V.: Hail metrics using conventional radar, in: *Proc., 16th Conference on Planned and Inadvertent*
420 *Weather Modification*, 2005.
- Forcadell, V., Augros, C., Caumont, O., Dedieu, K., Ouradou, M., David, C., Figueras i Ventura, J., Laurantin, O., and Al-Sakka, H.: Severe hail detection with C-band dual-polarisation radars using convolutional neural networks, *EGUsphere*, 2024, 1–43, 2024.
- Gauthier, M. L., Petersen, W. A., Carey, L. D., and Christian Jr, H. J.: Relationship between cloud-to-ground lightning and precipitation ice mass: A radar study over Houston, *Geophysical research letters*, 33, 2006.
- 425 Handwerker, J.: Cell tracking with TRACE3DA new algorithm, *Atmospheric Research*, 61, 15–34, 2002.
- Heinselman, P. L. and Ryzhkov, A. V.: Validation of polarimetric hail detection, *Weather and forecasting*, 21, 839–850, 2006.
- Hohl, R., Schiesser, H.-H., and Aller, D.: Hailfall: the relationship between radar-derived hail kinetic energy and hail damage to buildings, *Atmospheric Research*, 63, 177–207, 2002.

- Holleman, I., Wessels, H., Onvlee, J., and Barlag, S.: Development of a hail-detection-product: S10: Deep convection, Physics and Chemistry of the Earth, Part B: Hydrology, Oceans and Atmosphere, 25, 1293–1297, 2000.
- Junghänel, T., Brendel, C., Winterrath, T., and Walter, A.: Towards a radar-and observation-based hail climatology for Germany, Meteorol. Z, 25, 435–445, 2016.
- Kaltenböck, R., Diendorfer, G., and Dotzek, N.: Evaluation of thunderstorm indices from ECMWF analyses, lightning data and severe storm reports, Atmospheric Research, 93, 381–396, 2009.
- McGovern, A., Ebert-Uphoff, I., Gagne, D. J., and Bostrom, A.: Why we need to focus on developing ethical, responsible, and trustworthy artificial intelligence approaches for environmental science, Environmental Data Science, 1, 2022.
- Mirkovic, D. and Zrnica, D. S.: Library of rough hailstone backscattering coefficients at 2.8 GHz, Scientific Data, 10, 456, 2023.
- Mosier, R. M., Schumacher, C., Orville, R. E., and Carey, L. D.: Radar nowcasting of cloud-to-ground lightning over Houston, Texas, Weather and Forecasting, 26, 199–212, 2011.
- Murillo, E. M. and Homeyer, C. R.: Severe hail fall and hailstorm detection using remote sensing observations, Journal of applied meteorology and climatology, 58, 947–970, 2019.
- Nisi, L., Martius, O., Hering, A., Kunz, M., and Germann, U.: Spatial and temporal distribution of hailstorms in the Alpine region: a long-term, high resolution, radar-based analysis, Quarterly Journal of the Royal Meteorological Society, 142, 1590–1604, 2016.
- Pučík, T., Castellano, C., Groenemeijer, P., Kühne, T., Rädler, A. T., Antonescu, B., and Faust, E.: Large hail incidence and its economic and societal impacts across Europe, Monthly Weather Review, 147, 3901–3916, 2019.
- Puskeiler, M.: Radarbasierte Analyse der Hagelgefährdung in Deutschland, vol. 59, KIT Scientific Publishing, 2014.
- Puskeiler, M., Kunz, M., and Schmidberger, M.: Hail statistics for Germany derived from single-polarization radar data, Atmospheric Research, 178, 459–470, 2016.
- Reinert, D., Prill, F., Frank, H., Denhard, M., Baldauf, M., Schraff, C., Gebhardt, C., Marsigli, C., and Zängl, G.: DWD database reference for the global and regional ICON and ICON-EPS forecasting system, DWD 2023 Available online: [https://www.dwd.de/DWD/forschung/nwv/fepub/icon database main. pdf](https://www.dwd.de/DWD/forschung/nwv/fepub/icon%20database%20main.pdf) (accessed on 27 January 2023), 2020.
- Ryzhkov, A. V., Kumjian, M. R., Ganson, S. M., and Zhang, P.: Polarimetric radar characteristics of melting hail. Part II: Practical implications, Journal of Applied Meteorology and Climatology, 52, 2871–2886, 2013.
- Sánchez, J., Fraile, R., De La Madrid, J., De La Fuente, M., Rodríguez, P., and Castro, A.: Crop damage: The hail size factor, Journal of Applied Meteorology and Climatology, 35, 1535–1541, 1996.
- Schmid, T., Portmann, R., Villiger, L., Schröer, K., and Bresch, D. N.: An open-source radar-based hail damage model for buildings and cars, Natural Hazards and Earth System Sciences Discussions, 2023, 1–38, 2023.
- Snyder, J. C., Ryzhkov, A. V., Kumjian, M. R., Khain, A. P., and Picca, J.: A ZDR column detection algorithm to examine convective storm updrafts, Weather and Forecasting, 30, 1819–1844, 2015.
- Snyder, J. C., Bluestein, H. B., Dawson II, D. T., and Jung, Y.: Simulations of polarimetric, X-band radar signatures in supercells. Part II: Z DR columns and rings and K DP columns, Journal of Applied Meteorology and Climatology, 56, 2001–2026, 2017.
- Spitzer, A., Kempf, H., Jerg, M., and Blahak, U.: DWD-Crowdsourcing: User Reports available on Open Data, Tech. rep., Copernicus Meetings, 2023.
- Trefalt, S., Germann, U., Hering, A., Clementi, L., Boscacci, M., Schröer, K., and Schwierz, C.: Hail Climate Switzerland Operational radar hail detection algorithms at MeteoSwiss: quality assessment and improvement, Tech. Rep. 284, MeteoSwiss, <https://doi.org/10.18751/PMCH/TR/284.HailClimateSwitzerland/1.0>, 2022.

- Uber Technologies Inc.: H3: A hexagonal hierarchical geospatial indexing system, <https://h3geo.org/>, 2018.
- Waldvogel, A., Federer, B., and Grimm, P.: Criteria for the detection of hail cells, *Journal of Applied Meteorology and Climatology*, 18, 1521–1525, 1979.
- 470 Wilhelm, L., Schwierz, C., Schröer, K., Taszarek, M., and Martius, O.: A modelled multi-decadal hailday time series for Switzerland, *EGUsphere*, 2024, 1–57, 2024.
- Witt, A., Eilts, M. D., Stumpf, G. J., Johnson, J., Mitchell, E. D. W., and Thomas, K. W.: An enhanced hail detection algorithm for the WSR-88D, *Weather and Forecasting*, 13, 286–303, 1998.